Research Article Vol. 2, No. 2 / 15 February 2019 / OSA Continuum 314

Compensating chirp of attosecond X-ray pulses by a neutral hydrogen gas

ZENGHU CHANG*

Institute for the Frontier of Attosecond Science and Technology, CREOL and Department of Physics, University of Central Florida, 4111 Libra Drive, PS430, Orlando, FL 32816, USA
*Zenghu.Chang@ucf.edu

Abstract: It is demonstrated by numerical simulations that the attosecond chirp of high order harmonic pulses in the 530 to 1000 eV range can be partially compensated by the negative group delay dispersion of unionized molecular hydrogen gas. The transmission of X-rays through gas with the required pressure-length product for optimum chirp compensation is higher than 10% in the photon energy range that covers the K-edge of oxygen and L-edges of iron, cobalt, and nickel.

1. Introduction

When an X-ray beam interacts with magnetic matter, a strong magnetization-sensitive response can arise if the spin-orbit interaction plays an important role. This is typically the case for core-levels of transition metal elements when the X-ray energy is tuned to their transition energies. Attosecond X-ray pulses in the 700 to 900 eV range based on high harmonic generation (HHG) may play an important role in studying electron dynamics in ferromagnetic magnet materials that contain transition metal elements, Fe, Co and Ni. The absorption edges of these elements are 708.1 eV (Fe L_2), 721.1 eV (Fe L_1), 778.6 eV (Co L_2), 793.8 eV (Co L_1), 854.7 (Ni L_2), and 871.9 eV (Ni L_1). Attosecond X-rays covering the K-edge of Oxygen at 532.0 eV may serve as probes to observe charge migration in molecules [1].

High-order harmonic generation was first demonstrated in the late 1980s, which laid the foundation for table-top coherent ultrafast X-ray sources. At the present time, extreme ultraviolet (XUV) pulses with sufficient flux in the 10 to 150 eV range for transient absorption and other experiments can be reliably generated from noble gases interacting with near-infrared (NIR) Ti:Sapphire lasers centered at 800 nm [2]. In 1993, the mechanism of the high harmonic generation was explained by a three-step model [3,4]. It predicts that the cut-off photon energy is proportional to the square of the driving laser wavelength. Extending the cut-off by increasing the driving laser wavelength was first demonstrated with a Ti:Sapphire pumped Optical Parametric Amplifier (OPA) at 1.5 μm [5]. Recently, high flux high harmonic spectra in the water window (282 to 533 eV) have been achieved by using lasers with 1.6 to 2 μm center wavelengths [6]. Isolated 53-as soft X-ray pulses reaching the Carbon K-edge (282 eV) have been produced using a 1.7 μm laser [7]. For generating high harmonics in the 530 to 1 keV region by interacting helium atoms with laser pulses centered at 3.2 μm [8], the peak intensity of the mid-infrared (MIR) laser needs to be $\sim 4 \times 10^{14}$ W/cm^2.

The attosecond chirp (atto-chirp) of high harmonic pulses corresponding to the short trajectory is positive. Its value at the center of the plateau region may be estimated by [9],

$$Chirp = 1.63 \times 10^{18} \frac{1}{I_0 \lambda_0}. \quad (1)$$

The unit of the chirp is as^2, and the units of I_0 and λ_0 are W/cm^2 and eV respectively. The chirp is 1273 as^2 when the 3.2 μm MIR driving laser intensity is at 4×10^{14} W/cm^2.

The atto-chirp in the 20 to 300 eV photon energy range can be compensated by the negative group delay dispersion (GDD) of thin metal foils, Al, Be, Cr and Sn or neutral gases, Ar and Xe

#351826 https://doi.org/10.1364/OSAC.2.000314
Journal © 2019 Received 14 Nov 2018; revised 19 Dec 2018; accepted 20 Dec 2018; published 28 Jan 2019

OSA CONTINUUM

[10]. The attosecond chirp in the water window (282 to 533 eV) may be partially removed by fully ionized hydrogen or helium plasma [11]. We illustrate in this report that atto-chirp in the 530 to 1000 eV range can be significantly reduced by unionized hydrogen gas with the proper pressure-length product and the transmission of the gas is higher than 10%.

2. Dispersion of neutral H_2 gas in the soft X-ray region

The complex index of refraction of neutral molecular hydrogen gas with number density N at the soft X-ray wavelength λ_x can be calculated by

$$\tilde{n}(\lambda_x) = 1 - \frac{1}{2\pi} N r_0 \lambda_x^2 [f_1(\lambda_x) + i f_2(\lambda_x)], \tag{2}$$

where r_0 is the classical electron radius. f_1 and f_2 are the semi-empirical atomic scattering factors, whose value can be downloaded from [12]. The group delay dispersion can be calculated from the real part of $\tilde{n}$.

The index of refraction can also be obtained from the Lorentz classical electron oscillator model with J resonant frequencies, ω_{0j},

$$\tilde{n}(\omega_x) = \sqrt{1 + \sum_{j=1}^{J} \frac{F_j \omega_{0j}^2}{\omega_{0j}^2 - \omega_x^2 + i\gamma_j \omega_x}}, \tag{3}$$

where ω_x is the angular frequency of the X-ray. F_j is the oscillator strength. γ_j is the damping rate, which is related to the width of the resonances.

For X-rays with photon energy higher than 530 eV, $\omega_x >> \omega_{0j}$ and $\omega_x >> \gamma_j$, the bound electrons behave as free particles, thus the real index of refraction is the same as the fully ionized hydrogen plasma

$$n(\omega_x) = \sqrt{1 - \frac{\omega_p^2}{\omega_x^2}}, \tag{4}$$

where ω_p is the angular frequency of the plasma, which can be determined by the number density of electrons,

$$\omega_p = \sqrt{\frac{e^2 N_e}{\varepsilon_0 m_e}}, \tag{5}$$

where $N_e = 2N$ is the electron number density for molecular hydrogen. e and m_e are the charge and mass of the electron respectively. ε_0 is the permittivity of free space.

For the plasma density considered here, $\omega_x >> \omega_p$,

$$n(\omega_x) \approx 1 - \frac{1}{2}\frac{\omega_p^2}{\omega_x^2}. \tag{6}$$

The real index of refraction calculated from Eqs. (2) and (6) are the same in the 530 to 1000 eV region.

The group delay dispersion (GDD) of a molecular hydrogen gas with length L is

$$GDD(\hbar\omega_x) = -\frac{e^2\hbar^3}{\varepsilon_0 m_e c}\frac{N_e L}{(\hbar\omega_x)^3} \tag{7}$$

Apparently it is the electron density-length product that determines the GDD value.

The particle number density of a standard gas at 1 atmosphere pressure and room temperature is $2.5 \times 10^{19}/\text{cm}^3$. For H_2 molecules with 5 atm pressure, $N_e = 2.5 \times 10^{20}/\text{cm}^3$. The GDD of

OSA CONTINUUM

such plasma with $L = 10$ cm is -180 as^2 at $\hbar\omega_x = 750$ eV, which can be used to compensate the atto-chirp of the X-ray pulses generated by a 3.2 μm laser. The length of the gas for compensating a 1273 as^2 chirp at 750 eV is about 70.6 cm. Molecular hydrogen is preferred because of the low absorption in the soft X-ray region as compared to other materials.

To generate high harmonics beyond the Oxygen K-edge with mid-infrared lasers, noble gas targets with large pressure-length products are needed to achieve high photon flux. The maximum pressure-length product is limited by X-ray absorption under the phase-match conditions. For instance, when helium is used, the pressure-length product should not be larger than 70 atm-cm to efficiently generate 530 eV photons. The GDD of a target with such a pressure-length product is also negative but the absolute value is much smaller than that of the atto-chirp.

3. Numerical simulations of chirp compensation

Numerical simulations based on the Strong Field Approximation of high harmonic generation [13] have been performed to demonstrate feasibility of the atto-chirp compensation in the 530 to 1000 eV photon energy region by the dispersion of unionized molecular hydrogen gas. The time domain dipole moment of a single helium atom interacting with a MIR laser pulse was calculated using the open-source code, HHGmax [13]. The dipole matrix element is hydrogen-like and the ionization potential is 24.59 eV. The contribution from the long trajectory is suppressed by properly setting the integration and window parameters in the code. The pulsed external laser field centered at 3.2 μm has a Gaussian temporal profile, as shown in Fig. 1. The FWHM duration, carrier envelope phase (CEP) and peak intensity are 11 fs, $5\pi/8$ rad, and 4×10^{14} W/cm^2 respectively. The pulse duration and CEP values are chosen to demonstrate the generation of single isolated attosecond pulses with the amplitude gating [14]. The particular carrier-envelope phase favors the generation of the broadest continuous X-ray spectrum.

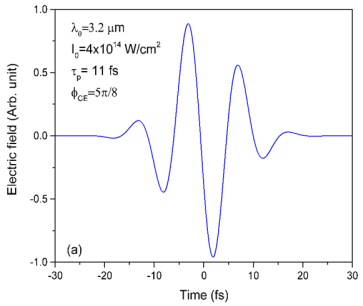

Fig. 1. Single-cycle mid-infrared driving laser field centered at 3.2 μm. The peak intensity is 4×10^{14} W/cm^2. The carrier envelope phase is $5\pi/8$ rad.

The power spectrum of the high harmonic pulse is shown in Fig. 2(a), which includes the effects of absorption of molecular hydrogen gas with 5 atm pressure and 77 cm in length. The transmission of the gas increases from 10% at 530 eV to 75% at 1000 eV, as illustrated in Fig. 2(b), which is obtained from [12] and is comparable to that of the materials used in XUV chirp compensation. The spectrum below 530 eV was set to zero to show the effects of atto-chirp on the temporal profile of the X-ray pulse in the 530 to 1000 eV range.

The quadratic phase of the X-ray directly from the atom (without chirp compensation) reveals a positive chirp, as illustrated in Fig. 2(c). When the phase of a 77 cm long molecular hydrogen gas with 5 atm pressure is added to the high harmonic phase, the chirp is significantly reduced, which can be seen by the close to flat total phase in Fig. 2(c). The chirp compensation is not perfect and the shape the total phase curve suggests that the remaining phase errors are dominated by the 3rd order dispersion. The electron pressure-length product value was chosen to yield the

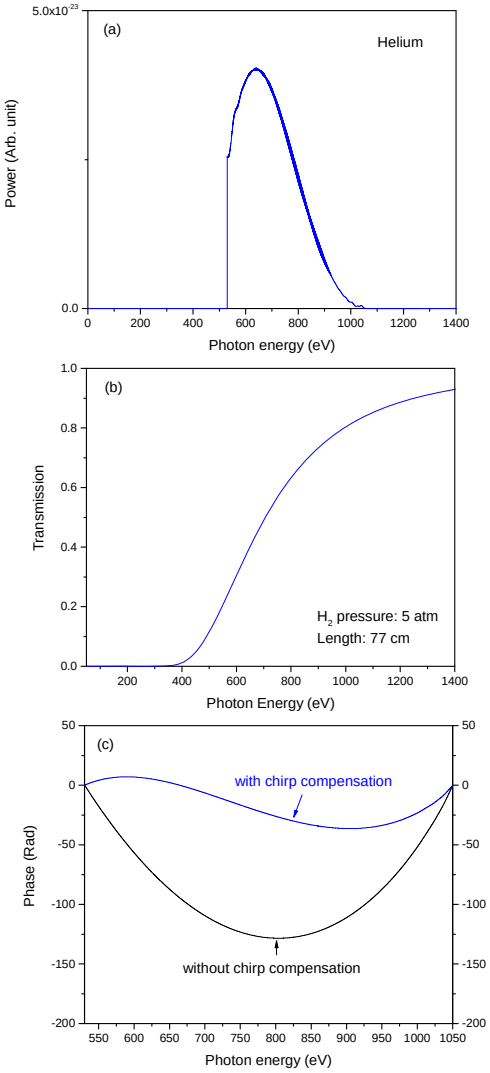

Fig. 2. (a) Power spectrum of the X-ray pulse. (b) Transmission of molecular hydrogen gas with pressure and length required for atto-chirp compensation. (c) Phases of X-rays with and without chirp compensation by the gas.

shortest compressed X-ray pulse. It is technically feasible to construct a gas filled tube that offers the required pressure-length product.

Without applying the chirp compensation, the electric field square of the X-ray pulse corresponding to the spectrum above 530 eV is illustrated in Fig. 3(a), which is 750-as long and far from being transform limited. When the gas phase is added, the X-ray pulse duration is reduced to 25 as, as a result of the atto-chirp compensation by the gas dispersion, as shown in Fig. 3(b). The duration of the transform limited X-ray pulse displayed in Fig. 3(c) is 7 as. The asymmetry of the waveform in Fig. 3(b) is due to the incompleteness of the chirp compensation. The multiple attosecond pulses at the trailing edge are caused by the third order phase error, as illustrated in Fig. 1 of [15].

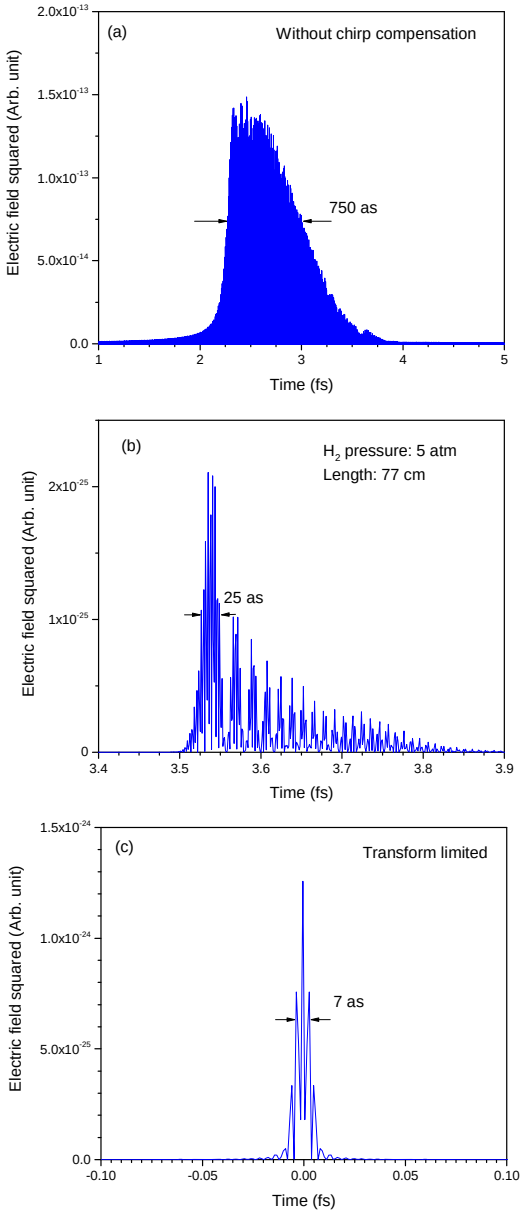

Fig. 3. Electric fields of the X-ray pulses. (a) Without chirp compensation. (b) With chirp compensation by hydrogen gas. (c) Transform-limited.

4. Summary

It is shown by numerical simulations that molecular hydrogen gas can effectively compress attosecond X-ray pulses in 530 to 1000 eV range. The X-ray transmission of a 77 cm long tube filled with unionized H_2 at 5 atmosphere pressure needed for atto-chirp compensation is > 10% for photon energy higher than 530 eV, which could be acceptable for some experiments. Although the same amount of GDD and much higher X-ray transmission can be achieved when the gas is fully ionized, it is easier to implement the chirp compensation with neutral gases since ionizing the gas with discharge requires high voltage and current. Both neutral hydrogen gas and

OSA CONTINUUM

plasma could be used at lower photon energy, such as in the water window, since the required pressure-length product is much smaller. They may be combined with other schemes to reduce atto-chirp when attosecond X-ray pulses are generated with either longer wavelength driving lasers or waveform synthesizers [16,17].

Funding

Air Force Office of Scientific Research (AFOSR) (FA9550-15-1-0037, FA9550-16-1-0013, FA9550-17-1-0499); Army Research Office (ARO) (W911NF-14-1-0383); Defense Advanced Research Projects Agency (DARPA) (D18AC00011); National Science Foundation Directorate for Mathematical and Physical Sciences (MPS) (1806584).

References

1. J. Breidbach and L. S. Cederbaum, "Migration of holes: Formalism, mechanisms, and illustrative applications," J. Chem. Phys. **118**(9), 3983–3996 (2003).
2. Z. Chang, P. B. Corkum, and S. R. Leone, "Attosecond optics and technology: progress to date and future prospects [Invited]," J. Opt. Soc. Am. B **33**(6), 1081–1097 (2016).
3. P. B. Corkum, "Plasma perspective on strong field multiphoton ionization," Phys. Rev. Lett. **71**(13), 1994 (2001).
4. K. Schafer, B. Yang, L. DiMauro, and K. Kulander, "Above threshold ionization beyond the high harmonic cutoff," Phys. Rev. Lett. **70**(11), 1599 (1993).
5. B. Shan and Z. Chang, "Dramatic extension of the high-order harmonic cutoff by using a long-wavelength driving field," Phys. Rev. A **65**(1), 011804 (2001).
6. X. Ren, J. Li, Y. Yin, K. Zhao, A. Chew, Y. Wang, S. Hu, Y. Cheng, E. Cunningham, and Y. Wu, "Attosecond light sources in the water window," J. Opt. **20**(2), 023001 (2018).
7. J. Li, X. Ren, Y. Yin, K. Zhao, A. Chew, Y. Cheng, E. Cunningham, Y. Wang, S. Hu, Y. Wu, M. Chini, and Z. Chang, "53-attosecond X-ray pulses reach the carbon K-edge," Nat. Commun. **8**(1), 186 (2017).
8. Y. Yin, J. Li, X. Ren, Y. Wang, A. Chew, and Z. Chang, "High-energy two-cycle pulses at 3.2 μm by a broadband-pumped dual-chirped optical parametric amplification," Opt. Express **24**(22), 24989–24998 (2016).
9. Z. Chang, "Fundamentals of Attosecond Optics," CRC Press, ISBN 9781420089370 (2011).
10. K. T. Kim, C. M. Kim, M.-G. Baik, G. Umesh, and C. H. Nam, "Single sub− 50− attosecond pulse generation from chirp-compensated harmonic radiation using material dispersion," Phys. Rev. A **69**(5), 051805 (2004).
11. Z. Chang, "Attosecond chirp compensation in water window by plasma dispersion," Opt. Express **26**(25), 33238–33244 (2018).
12. E. Gullikson, http://henke.lbl.gov/optical_constants/asf.html.
13. M. Hoegner, https://github.com/Leberwurscht/HHGmax.
14. M. Chini, K. Zhao, and Z. Chang, "The generation, characterization and applications of broadband isolated attosecond pulses," Nat. Photonics **8**(3), 178–186 (2014).
15. A. V. Dostovalov, A. A. Wolf, S. A. Babin, M. V. Dubov, and V. K. Mezentsev, "Numerical investigation of the effect of the temporal pulse shape on modification of fused silica by femtosecond pulses," Quantum Electron. **42**(9), 799–804 (2012).
16. Y. Fu, H. Yuan, K. Midorikawa, P. Lan, and E. J. Takahashi, "Towards GW-scale isolated attosecond pulse far beyond carbon K-edge driven by mid-infrared waveform synthesizer," Appl. Sci. **8**(12), 2451 (2018).
17. Z. Zeng, Y. Zheng, Y. Cheng, R. Li, and Z. Xu, "Attosecond pulse generation driven by a synthesized laser field with two pulses of controlled related phase," J. Phys. B: At., Mol. Opt. Phys. **45**(7), 074004 (2012).